Cluster Compounds

DOI: 10.1002/ange.200502678

Observation of d-Orbital Aromaticity**

*Xin Huang, Hua-Jin Zhai, Boggavarapu Kiran, and Lai-Sheng Wang**

Aromaticity is one of the most important concepts in chemistry and refers to planar cyclic hydrocarbon molecules that exhibit delocalized π-bonds and unusual stability, such as benzene. This concept has been extended to metal-substituted organic molecules,[1,2] as well as main group organometallic complexes.[3–6] The recent discovery of aromaticity in all-metal clusters, for instance $[Al_4]^{2-}$ in $[MAl_4]^-$ (M = Cu, Li, Na),[7] has led to a flurry of research activities[8–16] and predictions of new aromatic metal clusters,[17–23] among which is a class of interesting cyclic species containing Cu.[20,23]

While main group clusters can give rise to σ- and π-aromaticity, transition-metal-containing clusters can exhibit d-orbital aromaticity or, more interestingly, δ-aromaticity due to δ bonding interactions. However, d-orbital aromaticity requires significant d–d bonding interactions. Unlike valent s or p orbitals, d orbitals are spatially more contracted, and their tendency to participate in chemical bonding depends strongly on the position of the transition metals in the periodic table and their coordination environments. The predicted aromaticity in the cyclic Cu-containing species,[20,23] for example, has not been verified experimentally. More promisingly, d-orbital aromaticity is expected to be found in early or 4d/5d transition metal systems, where strong d–d interactions are known. Here, we report experimental and theoretical evidence of d-orbital aromaticity in two early 4d and 5d transition metal oxide clusters, namely $[M_3O_9]^-$ and $[M_3O_9]^{2-}$ (M = W, Mo).

[*] Dr. X. Huang, Dr. H.-J. Zhai, Dr. B. Kiran, Prof. Dr. L.-S. Wang
Department of Physics
Washington State University
2710 University Drive, Richland, WA 99354 (USA)
and
W. R. Wiley Environmental Molecular Sciences Laboratory and
Chemical Sciences Division
Pacific Northwest National Laboratory
P.O. Box 999, Richland, WA 99352 (USA)
Fax: (+1) 509-376-6066
E-mail: ls.wang@pnl.gov

[**] We thank Prof. A. I. Boldyrev, Dr. Jun Li, and Dr. Tom Waters for valuable discussions. This work was supported by the Chemical Sciences, Geosciences, and Biosciences Division of the Office of Basic Energy Sciences, U.S. Department of Energy (DOE) under grant number DE-FG02-03ER15481 (catalysis center program) and was performed at the W. R. Wiley Environmental Molecular Sciences Laboratory (EMSL), a national scientific user facility sponsored by DOE's Office of Biological and Environmental Research and located at Pacific Northwest National Laboratory, operated for DOE by Battelle. Calculations were performed at the EMSL Molecular Science Computing Facility.

Supporting information for this article is available on the WWW under http://www.angewandte.org or from the author.

© 2005 Wiley-VCH Verlag GmbH & Co. KGaA, Weinheim

Early transition metal oxide clusters have recently gained experimental and theoretical attention due to their importance in catalysis.[24–26] We investigated the structure and bonding of early transition metal oxide clusters using a combined photoelectron spectroscopy (PES) and theoretical approach with the aim of discovering specific structures or clusters that may mimic a catalytic site.[27,28] Our experiment was carried out with a magnetic-bottle PES apparatus with a laser vaporization cluster source. A pure metal target (W or Mo) was used in the laser vaporization with a helium carrier gas containing 0.5% O_2. $[M_xO_y]^-$-type clusters with various stoichiometry were produced from reactions between the laser-induced plasma and O_2 in the carrier gas and were separated in a time-of-flight mass spectrometer. The $[M_3O_9]^-$ clusters (M = W, Mo) of interest were selected and decelerated before being intercepted by a 157-nm laser beam from an F_2 excimer laser. Photoemitted electrons were collected by a magnetic bottle with nearly 100% efficiency and analyzed in a 3.5-m-long electron flight tube. The photoelectron spectra were calibrated against the known spectrum of Rh^- and the apparatus had an electron energy resolution of $\Delta E_k/E_k \approx 2.5\%$, i.e., approximately 25 meV for 1-eV electrons.

Figure 1 displays the 157-nm spectra of $[W_3O_9]^-$ and $[Mo_3O_9]^-$, which are similar, each with a weak and broad threshold band (X) followed by a large energy gap and more features at very high electron-binding energies. The X band in both spectra yields a similar threshold detachment energy of about 3.5 eV for $[W_3O_9]^-$ and $[Mo_3O_9]^-$, and vertical detachment energies (VDEs) of 4.2 and 4.0 eV, respectively. The neutral $[M_3O_9]$ clusters are stoichiometric species in which W and Mo assume their highest oxidation state, M^{6+}. Thus, the threshold band (X) should correspond to detachment of the extra electron in the anions that occupies an d-type orbital that is empty in the neutral species, whereas the higher detachment features should all derive from detachment from O 2p-type orbitals. Interestingly, the observed energy gaps in the photoelectron spectra (Figure 1) of about 3.3 eV (3.2 eV) for $[W_3O_9]^-$ ($[Mo_3O_9]^-$), are already very close to that for the corresponding bulk MO_3 oxides. The threshold band (X) in both spectra is extremely broad, in particular in the spectrum of $[W_3O_9]^-$, thus suggesting that there is a large difference in geometry between the anion and neutral ground state of the $[M_3O_9]$ clusters.

To understand the structures and bonding in the $[M_3O_9]$ and $[M_3O_9]^-$ clusters, we carried out density functional theory (DFT) calculations.[29] Figure 2 displays the ground-state structures for $[M_3O_9]$ and $[M_3O_9]^-$. The structures of neutral $[W_3O_9]$ and $[Mo_3O_9]$ are nearly identical, with D_{3h} symmetry, and each metal atom is bonded to two bridging O atoms and two terminal O atoms. The $[W_3O_9]^-$ and $[Mo_3O_9]^-$ anions also display D_{3h} symmetry, but the M–M distance is significantly reduced by 0.29 Å in $[W_3O_9]^-$ and 0.25 Å in $[Mo_3O_9]^-$ relative to the neutral structures, and this is accompanied by a large increase in the OMO angle and a large decrease in the MOM angle that makes the M_3O_3 ring almost a perfect hexagon in $[M_3O_9]^-$ (Figures 2b and 2e). These geometrical changes are consistent with the broad ground-state PES band for the two clusters (Figure 1). Our calculated VDEs of 4.39 and 4.11 eV agree well with the measured values of 4.2 and 4.0 eV for $[W_3O_9]^-$ and $[Mo_3O_9]^-$, respectively, and our calculated adiabatic detachment energies (ADEs) for the two anions are 3.0 eV, which is smaller than the experimental threshold value of 3.5 eV. The large differences between the calculated ADEs and VDEs are consistent with the large difference in geometry between the anion and neutral ground-states. The smaller value of the calculated ADE relative to the experimental threshold value suggests that the 0–0 transition from the ground state of the anion to that of the neutral clusters may have negligible Franck–Condon factors due to the large difference in geometry, and the measured threshold detach-

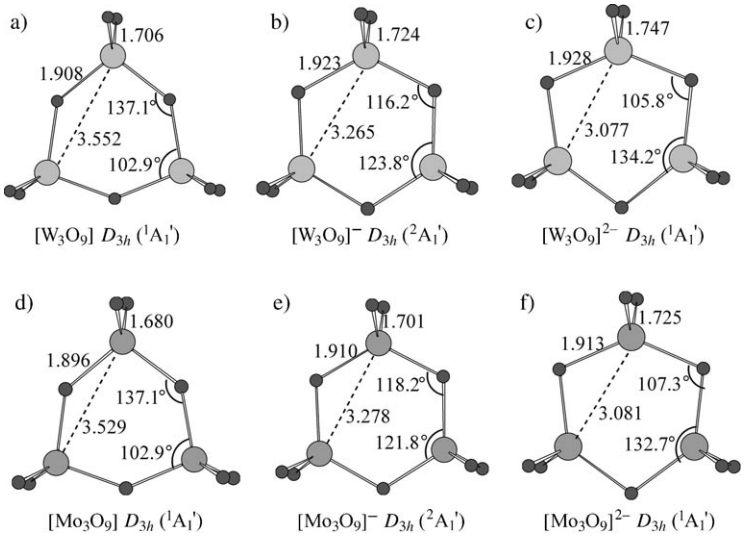

Figure 2. Optimized structures for $[M_3O_9]$, $[M_3O_9]^-$, and $[M_3O_9]^{2-}$ (M = W and Mo).

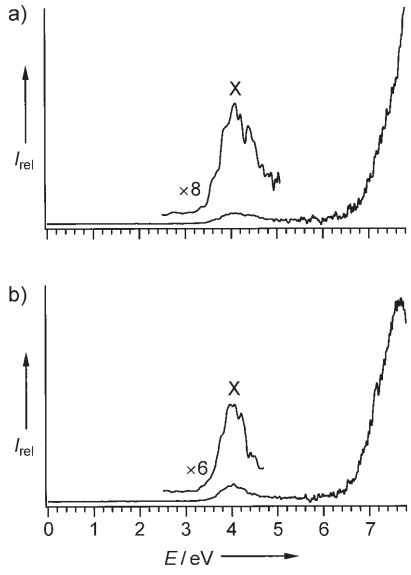

Figure 1. Photoelectron spectra of $[W_3O_9]^-$ (a) and $[Mo_3O_9]^-$ (b) at 157 nm (7.866 eV).

 © 2005 Wiley-VCH Verlag GmbH & Co. KGaA, Weinheim

ment energy can only serve as an upper limit for the true adiabatic value.

The surprisingly large geometry change induced by addition of a single electron to $[M_3O_9]$ suggests that the molecular orbital that the extra electron occupies in the anion must involve strong metal–metal bonding. Figures 3a and 3b

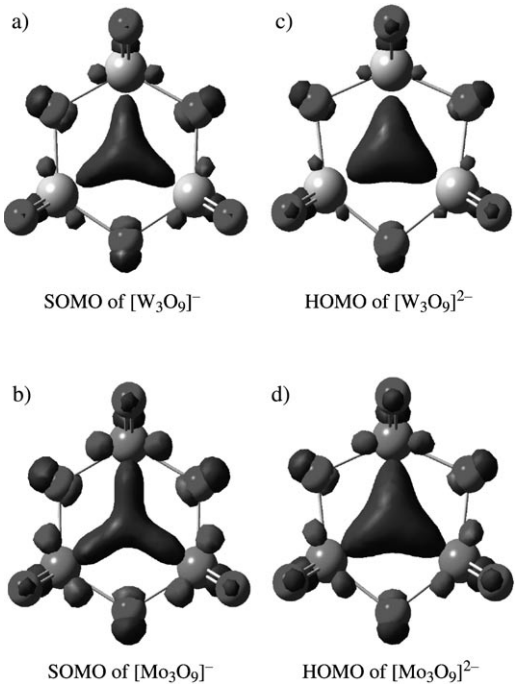

Figure 3. The singly occupied molecular orbital (SOMO) for $[W_3O_9]^-$ (a) and $[Mo_3O_9]^-$ (b) and the highest occupied molecular orbital (HOMO) of $[W_3O_9]^{2-}$ (c) and $[Mo_3O_9]^{2-}$ (d).

show the singly occupied molecular orbitals (SOMOs) for $[M_3O_9]^-$, which indeed describe nearly pure three-center M–M σ-bonding interactions with very little contribution from the O atoms. Judging by the huge M–M distance change induced by the single electron, these SOMOs must depict two strong three-center, one-electron (3c–1e) metal–metal bonds. The SOMO of $[M_3O_9]^-$ is a nondegenerate a_1' orbital. Addition of a second electron to this a_1' orbital gives rise to closed-shell $[M_3O_9]^{2-}$ dianions, which also display D_{3h} symmetry (Figure 2c, f) and a three-center, two-electron (3c–2e) bond (Figures 3c and 3d). Our calculations show that the dianions are also unusually stable despite the strong intramolecular coulomb repulsion. In fact, $[W_3O_9]^{2-}$ is predicted to be a stable gas-phase dianion with a calculated electron binding energy of 0.03 eV relative to $[W_3O_9]^-$. The $[Mo_3O_9]^{2-}$ dianion is predicted to be slightly unstable, with a small negative electron binding energy of −0.14 eV. More significantly, we found that the addition of a second electron to $[M_3O_9]^-$ also induces a considerable shortening of the M–M bond length of 0.19 Å (0.20 Å) for $[W_3O_9]^{2-}$ ($[Mo_3O_9]^{2-}$) relative to $[M_3O_9]^-$.

To gain further insight into the 3c–1e and 3c–2e bonds in $[M_3O_9]^-$ and $[M_3O_9]^{2-}$, we estimated their resonance energies (see Supporting Information).[30] Two isodesmic equations were used for $[W_3O_9]^{2-}$ to eliminate the potential influence of the different electrostatic interactions in the doubly charged anions. When the intramolecular coulomb interactions of the dianions involved are balanced by the K^+ cation a very large resonance energy of 1.05 eV is obtained, which is, in fact, comparable to the value estimated for benzene.[30] This large resonance energy suggests that the $[M_3O_9]^{2-}$ species may be viewed as highly aromatic. We further calculated their nucleus independent chemical shifts (NICS), which have been suggested as a magnetic criterion for aromaticity.[31] We obtained NICS values of −21.5 and −20.5 at the ring center for $[W_3O_9]^{2-}$ and $[Mo_3O_9]^{2-}$, respectively (see Supporting Information), that are much higher than those predicted for the cyclic Cu-containing clusters[20,23] and are comparable to the multiply aromatic $[Al_4]^{2-}$. The large resonance energies, the equal M–M bond lengths, and the large negative NICS values all suggest that $[W_3O_9]^{2-}$ and $[Mo_3O_9]^{2-}$ are highly aromatic species. More interestingly, we also obtained a sizable resonance energy for $[W_3O_9]^-$ (0.33 eV, see Supporting Information) even though it only contains a single delocalized electron, which suggests it may also be considered as aromatic; this was corroborated by the NICS values.

Trinuclear clusters of W and Mo have been studied extensively.[32,33] However, all these cluster complexes involve M^{4+} metal centers, typified by the $[M_3O_4]^{4+}$ core, whose metal–metal bonding can be described by three classical 2c–2e metal–metal bonds; they are therefore not expected to exhibit aromaticity. Quasi-aromaticity has been invoked to explain the strong M–O interactions in the $[M_3O_4]^{4+}$-type complexes,[34,35] but that is very different from the d-orbital aromaticity in the $[M_3O_9]^-$ and $[M_3O_9]^{2-}$ clusters discussed here. Aromaticity has also been considered in trinuclear Pt_3 and Os_3 metal complexes solely on the basis of molecular orbital topologies,[36,37] but it has not been verified using other criteria for aromaticity.

The $[M_3O_9]^-$ and $[M_3O_9]^{2-}$ clusters described here are unique in that they involve a single, fully delocalized metal–metal bond and may be considered as a new class of d-orbital aromatic molecules. The oxidation state of M can be considered to be fractional— +17/3 in $[M_3O_9]^-$ and +16/3 in $[M_3O_9]^{2-}$. Polyoxometalate clusters involving W and Mo are also well known.[38] The high stability of the $[M_3O_9]^-$ and $[M_3O_9]^{2-}$ clusters suggest that they may also be synthesized in the condensed phase. With the extra delocalized d-electrons, these clusters may exhibit novel chemical, electrochemical, and catalytic properties.

Received: July 29, 2005
Published online: October 17, 2005

Keywords: aromaticity · cluster compounds · density functional calculations · metal–metal interactions · photoelectron spectroscopy

[1] J. R. Bleeke, *Chem. Rev.* **2001**, *101*, 1205.
[2] B. E. Bursten, R. F. Fenske, *Inorg. Chem.* **1979**, *18*, 1760.
[3] X. W. Li, W. T. Pennington, G. H. Robinson, *J. Am. Chem. Soc.* **1995**, *117*, 7578.
[4] Y. Xie, P. R. Schreiner, H. F. Schaefer III, X. W. Li, G. H. Robinson, *J. Am. Chem. Soc.* **1996**, *118*, 10635.

 © 2005 Wiley-VCH Verlag GmbH & Co. KGaA, Weinheim

[5] A. E. Kuznetsov, A. I. Boldyrev, X. Li, L. S. Wang, *J. Am. Chem. Soc.* **2001**, *123*, 8825.
[6] A. D. Phillips, P. P. Power, *J. Cluster Sci.* **2002**, *13*, 569.
[7] X. Li, A. E. Kuznetsov, H. F. Zhang, A. I. Boldyrev, L. S. Wang, *Science* **2001**, *291*, 859.
[8] P. W. Fowler, R. W. A. Havenoth, E. Steiner, *Chem. Phys. Lett.* **2001**, *342*, 85.
[9] X. Li, H. F. Zhang, L. S. Wang, A. E. Kuznetsov, N. A. Cannon, A. I. Boldyrev, *Angew. Chem.* **2001**, *113*, 1919; *Angew. Chem. Int. Ed.* **2001**, *40*, 1867.
[10] A. E. Kuznetsov, J. D. Corbett, L. S. Wang, A. I. Boldyrev, *Angew. Chem.* **2001**, *113*, 3473; *Angew. Chem. Int. Ed.* **2001**, *40*, 3369.
[11] A. I. Boldyrev, A. E. Kuznetsov, *Inorg. Chem.* **2002**, *41*, 532.
[12] C. G. Zhan, F. Zheng, D. A. Dixon, *J. Am. Chem. Soc.* **2002**, *124*, 14795.
[13] P. W. Fowler, R. W. A. Havenoth, E. Steiner, *Chem. Phys. Lett.* **2002**, *359*, 530.
[14] A. E. Kuznetsov, H. J. Zhai, L. S. Wang, A. I. Boldyrev, *Inorg. Chem.* **2002**, *41*, 6062.
[15] H. Tanaka, S. Neukemans, E. Janssens, R. E. Silverans, P. Lievens, *J. Am. Chem. Soc.* **2003**, *125*, 2862.
[16] J. C. Santos, W. Tiznado, R. Contreras, P. Fuentealba, *J. Chem. Phys.* **2004**, *120*, 1670.
[17] J. Juselius, M. Straka, D. Sundholm, *J. Phys. Chem. A* **2001**, *105*, 9939.
[18] X. X. Chi, X. H. Li, X. J. Chen, Z. S. Yuang, *J. Mol. Struct. (Theochem)* **2004**, *677*, 21.
[19] A. E. Kuznetsov, A. I. Boldyrev, *Struct. Chem.* **2002**, *12*, 141.
[20] A. C. Tsipis, C. A. Tsipis, *J. Am. Chem. Soc.* **2003**, *125*, 1136.
[21] J. M. Mercero, J. M. Ugalde, *J. Am. Chem. Soc.* **2004**, *126*, 3380.
[22] Q. Kong, M. Chen, J. Dong, Z. Li, K. Fan, M. Zhou, *J. Phys. Chem. A* **2002**, *106*, 11709.
[23] C. S. Wannere, C. Corminboeuf, Z. X. Wang, M. D. Wodrich, R. B. King, P. von R. Schleyer, *J. Am. Chem. Soc.* **2005**, *127*, 5701.
[24] H. T. Deng, K. P. Kerns, A. W. Castleman, Jr., *J. Phys. Chem.* **1996**, *100*, 13385.
[25] Q. Sun, B. K. Rao, P. Jena, D. Stolcic, Y. D. Kim, G. Gantefor, A. W. Castleman, Jr., *J. Chem. Phys.* **2004**, *121*, 9417.
[26] B. L. Yoder, J. T. Maze, K. Raghavachari, C. C. Jarrold, *J. Chem. Phys.* **2005**, *122*, 094313.
[27] H. J. Zhai, B. Kiran, L. F. Cui, X. Li, D. A. Dixon, L. S. Wang, *J. Am. Chem. Soc.* **2004**, *126*, 16134.
[28] H. J. Zhai, X. Huang, L. F. Cui, X. Li, J. Li, L. S. Wang, *J. Phys. Chem. A* **2005**, *109*, 6019.
[29] The theoretical calculations were performed at the DFT level using the B3LYP hybrid functional (A. D. Becke, *J. Chem. Phys.* **1993**, *98*, 1372). A number of possible structures were evaluated, and the search for the global minima and vibrational frequency calculations were performed using analytical gradients with the Stuttgart 14-valence-electron pseudo-potentials and the valence basis sets (D. Andrae, U. Haeussermann, M. Dolg, H. Stoll, H. Preuss, *Theor. Chim. Acta* **1990**, *77*, 123) augmented with two f-type and one g-type polarization functions for W ($\zeta(f)=0.256$, 0.825; $\zeta(g)=0.627$) for Mo and ($\zeta(f)=0.338$, 1.223; $\zeta(g)=$ 0.744), as recommended by Martin and Sundermann (J. M. L. Martin, A. Sundermann, *J. Chem. Phys.* **2001**, *114*, 3408), and the aug-cc-pVTZ basis set for oxygen (R. A. Kendall, T. H. Dunning, Jr., R. J. Harrison, *J. Chem. Phys.* **1992**, *96*, 6796). Scalar relativistic effects, i.e., the mass-velocity and Darwin effects, were taken into account by using the quasi-relativistic pseudopotentials. Vertical electron detachment energies (VDEs) were calculated using the generalized Koopman's theorem (D. J. Tozer, N. C. Handy, *J. Chem. Phys.* **1998**, *109*, 10180). The extra-fine integration grid was used to obtain accurate DFT results. The geometry optimizations and vibrational frequency analysis were accomplished with the NWChem 4.6 program (*NWChem, A Computational Chemistry Package for Parallel Computers, Version 4.6*: E. Aprà et al., see Supporting Information) and the Molecular Science Computing Facility located at the Environmental Molecular Sciences Laboratory. GaussView 3.0 was used to generate the three-dimensional contours of the calculated Kohn–Sham orbitals. Nucleus-independent chemical shifts (in ppm) were computed at the centers of the optimized structures using the GIAO-B3LYP (SDD for W and Mo, 6-31+G* for O) method with the Gaussian03 program (Gaussian03 (Revision B.04): M. J. Frisch et al., see Supporting Information).
[30] P. von R. Schleyer, H. Jiao, *Pure Appl. Chem.* **1996**, *68*, 209.
[31] P. von R. Schleyer, C. Maerker, A. Dransfeld, H. Jiao, N. J. R. van Eikema Hommes, *J. Am. Chem. Soc.* **1996**, *118*, 6317.
[32] A. Müller, R. Jostes, F. A. Cotton, *Angew. Chem.* **1980**, *92*, 921; *Angew. Chem. Int. Ed. Engl.* **1980**, *19*, 875.
[33] B. E. Bursten, F. A. Cotton, M. B. Hall, R. C. Najjar, *Inorg. Chem.* **1982**, *21*, 302.
[34] J. Li, C. W. Liu, J. X. Lu, *Polyhedron* **1994**, *13*, 1841.
[35] J. X. Lu, Z. D. Chen, *Int. Rev. Phys. Chem.* **1994**, *13*, 85.
[36] R. B. King, *Inorg. Chim. Acta* **2003**, *350*, 126.
[37] F. F. de Biani, A. Ienco, F. Laschi, P. Leoni, F. Marchetti, L. Marchetti, C. Mealli, P. Zanello, *J. Am. Chem. Soc.* **2005**, *127*, 3076.
[38] M. T. Pope, *Heteropoly and Isopoly Oxometalates*, Springer, Berlin, **1983**.

 © 2005 Wiley-VCH Verlag GmbH & Co. KGaA, Weinheim